THE JOURNAL OF PHYSICAL CHEMISTRY A

ARTICLE

pubs.acs.org/JPCA

Ultrafast Excited-State Dynamics of Eosin B: A Potential Probe of the Hydrogen-Bonding Properties of the Environment

Piotr Fita,† Marina Fedoseeva, and Eric Vauthey*

Department of Physical Chemistry, University of Geneva, 30 quai Ernest-Ansermet, CH-1211 Geneva 4, Switzerland

Supporting Information

ABSTRACT: The photophysics of two dyes from the xanthene family, eosin B (EB), and eosin Y (EY) has been investigated in various solvents by femtosecond transient absorption spectroscopy, first, to clarify the huge disparity of the EB fluorescence lifetimes reported in literature, and, second, to understand the mechanism responsible for the ultrafast excited-state deactivation of EB in water. The excited-state lifetime of EB was found to be much shorter in water and in other protic solvents, due to the occurrence of hydrogen-bond assisted nonradiative deactivation. This mechanism is associated with the hydrogen bonds between the solvent molecules and the nitro groups of EB, which become stronger upon optical excitation due to the charge-transfer character of the excited-state. This process is not operative with EY, where the nitro groups are replaced by bromine atoms. Therefore, the excited-state lifetime of EB in solution is directly related to the strength of the solvent as a hydrogen-bond donor, offering the possibility to build a corresponding scale based on the fluorescence quantum yield or lifetime of EB. This scale of hydrogen-bonding strength could be especially useful for studies of liquid interfaces by time-resolved surface second harmonic generation.

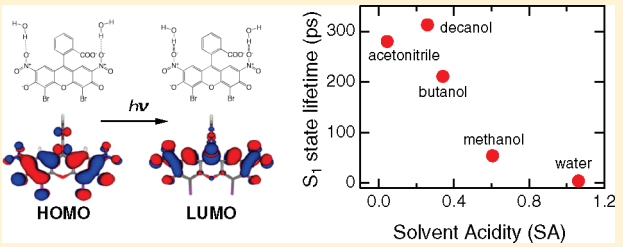

INTRODUCTION

Over the past several years, eosin B (EB, Figure 1), a dye from the xanthene family, has been successfully used in surface-second harmonic generation (SSHG) studies of acid−base equilibrium,[1] and orientational relaxation[2] at air/water interfaces. Although powerful by its surface-selectivity,[3−5] this technique provides data that are sometimes difficult to unambiguously interpret. Therefore, the picture of the interfacial dynamics of a probe is usually obtained by interpreting the SSHG data in light of the photophysics of the same probe in bulk solutions. Such comparison underlies the "dynamic probe" approach for studying interfaces by SSHG. A dynamic probe is a molecule, whose excited-state dynamics (for instance its S_1 lifetime) depends on properties of the environment, like, e.g., viscosity, polarity, or pH. As long as the dynamics of this molecule and its dependence on a given property of the environment is well characterized by bulk spectroscopy, the resonantly enhanced time-resolved SSHG (TRSSHG) can provide information on this property at the interface. This approach has been applied, for example, to malachite green for investigating friction at the interface.[6,7]

EB appears to be a convenient probe molecule for studying aqueous interfaces because it is water-soluble and its absorption spectrum allows its use in typical TRSSHG setups based on femtosecond Ti:Sapphire amplifiers. Despite this, very little is known about its photophysics in bulk solutions and the available data are contradictory. For instance, various sources report a S_1-state lifetime in alcohols going from 90 ps in methanol,[8] up to 4.5 and 5.3 ns in ethanol.[9−11] However, the lifetimes of the closely related eosin Y (EY, Figure 1) reported in literature are more consistent and vary from 1.1 ns in water to 3−4.5 ns in organic solvents.[9,12−14]

In order to clarify the excited-state dynamics of EB and understand its photophysics, which would greatly facilitate its application in TRSSHG studies of interfaces, we have carried out a series of femtosecond transient absorption measurements of both EB and EY in solution. We will show that EB is practically nonfluorescent in water and alcohols, in agreement with the work of Reindl and Penzkofer,[8] whereas EY is strongly fluorescent in all solvents investegated. The two dyes differ only by the presence of two nitro groups in EB that replace two of the four bromine atoms of EY. Therefore, the efficient radiationless deactivation of EB must be a direct consequence of this substitution. The present work reveals that the very short excited-state lifetime of EB in water and alcohols is due to the occurrence of hydrogen-bond assisted nonradiative deactivation. As a consequence, EB appears to be a valuable dynamic probe of the hydrogen-bonding properties in bulk environments and at liquid interfaces, as demonstrated by a recent TRSSHG study.[15]

EXPERIMENTAL SECTION

Samples. Eosin B (EB, disodium salt, Sigma-Aldrich) and eosin Y (EY, disodium salt, Acros Organics) were used without further purification. The organic solvents: methanol (MeOH,

Received: November 13, 2010
Revised: February 7, 2011
Published: March 07, 2011

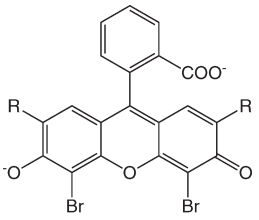

Eosin B (EB): R = NO_2
Eosin Y (RY): R = Br

Figure 1. Eosin B and eosin Y in their double anion form.

Acros Organics, p.a.), 1-butanol (BuOH, Merck, p.a.), 1-decanol (DeOH, Acros Organics, 99%), and acetonitrile (ACN, ROTH, ROTIDRY, > 99.9%, <10 ppm H_2O) were used as supplied. Deionized water was used for the aqueous solutions. Their pH was kept around 9−10 by addition of NaOH.

Steady-State Measurements. Absorption spectra were recorded on a Cary 50 spectrophotometer, whereas stationary fluorescence was measured on a Cary Eclipse fluorimeter. The fluorescence quantum yields were determined using rhodamine 6G in ethanol as a standard (Φ_{fl} = 0.95).[16]

Transient Absorption (TA). The experimental setup for TA spectroscopy has already been described in detail elsewhere.[17,18] Briefly, the excitation pulses were generated by a home-built noncollinear optical parametric amplifier (NOPA) fed by a standard Ti:Sapphire femtosecond amplified system (Spitfire, Spectra Physics) working at a 1 kHz repetition rate. The central wavelength of the pulses was at 520 nm, their duration was about 50 fs and the energy at the sample position was between 0.8 and 1.5 μJ. TA was probed at magic angle with white-light supercontinuum pulses generated in a 3-mm thick CaF_2 plate. After acquisition, all spectra were corrected for the chirp of the probe pulses. The samples were contained in a 1-mm thick fused silica cell and kept at room temperature. They were continuously stirred by bubbling with nitrogen. The response function of the setup had a width of about 200 fs.

Quantum Chemical Calculations. Ground-state gas-phase geometry optimization was performed at the density functional level of theory (DFT) using the B3LYP functional,[19] and a [3s2p1d] basis set.[20] Electronic vertical excitation energies were computed with time-dependent density functional theory (TD-DFT) using the same functional and basis set.[21] The calculations were carried out using Turbomole version 6.0.[22]

RESULTS AND DISCUSSION

Steady-State Spectroscopy. The study of the optical properties of the eosins is complicated by the existence of various forms in solutions: doubly charged anion (Figure 1), single anion (with the carboxyl group protonated), neutral and lactonic.[1] In aqueous solutions, the pK_a of the first and second dissociation steps are equal to, respectively, 2.2 and 3.7 for EB,[1] and 3.25 and 3.80 for EY.[23] Therefore, the pH of the aqueous solutions was kept above 8 to ensure that only the double-anion is present. This is confirmed by the absorption spectra measured in water at various pH, which do not change any more above a pH of 6 (Figure 2).

The absorption and fluorescence spectra of EB and EY in aqueous (at pH > 8) and MeOH solutions are shown in Figure 3, whereas the fluorescence quantum yields determined for EB in various solvents are listed in Table 1. The absorption spectra of both compounds are very similar and do not change significantly

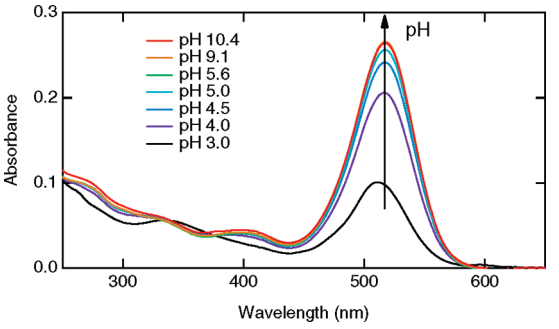

Figure 2. Steady-state absorption spectra of EB (7.10^{-6} M) at various pH.

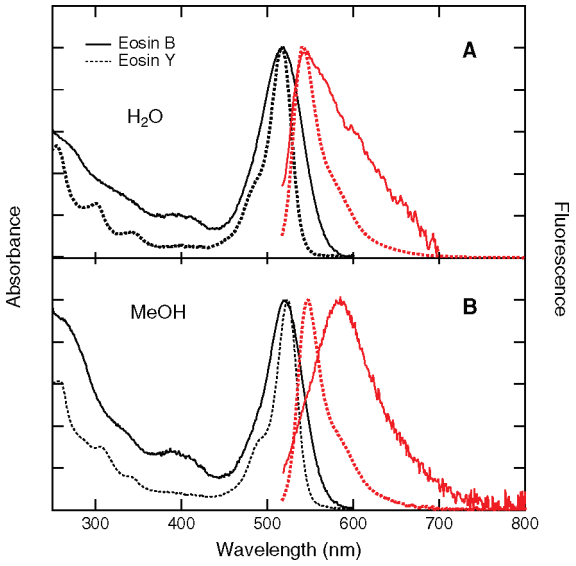

Figure 3. Steady-state absorption and fluorescence spectra of EB (solid line) and EY (dashed line) in (A) water and (B) MeOH.

Table 1. Fluorescence Quantum Yield of EB Measured in Various Solvents

solvent	Φ_{fl}
water	4.5×10^{-4}
methanol	7.5×10^{-3}
butanol	4.5×10^{-2}
decanol	6.6×10^{-2}
acetonitrile	3.6×10^{-2}

when going from water to MeOH. In longer alcohols, they are slightly red-shifted but otherwise do not differ from those in MeOH. This confirms that the dominating form of the molecules in alcoholic solutions is the double anion, the same as in basic aqueous solution. The emission spectrum of EY is mirror image of its absorption spectrum and the Stokes shift is relatively small, about 900 cm^{-1}. This is not the case with EB, whose emission spectrum is significantly broader and exhibits a bigger Stokes shift in MeOH (~2200 cm^{-1}). Surprisingly, the Stokes shift of EB in water is smaller than in MeOH. This stems from the extremely short fluorescence lifetime of EB in water which, as it will be shown below, amounts to a few picoseconds and accounts for the very small fluorescence quantum yield (Table 1). This lifetime is

dx.doi.org/10.1021/jp110849x |J. Phys. Chem. A 2011, 115, 2465–2470

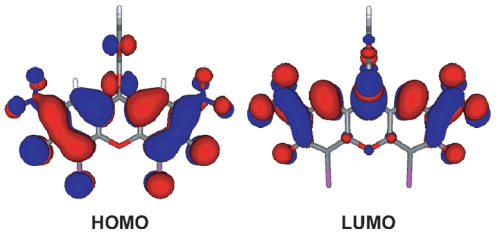

Figure 4. Frontier molecular orbitals of EB drawn at the 0.02 au level.

comparable to the time scale of solvent relaxation, meaning that fluorescence is due to partially nonequilibrated, not fully solvated molecules. As a consequence, the average emission is shifted to higher energies compared to MeOH, where the fluorescence lifetime is much longer.

The spectral differences between the dyes indicate that, contrary to EY, the emitting state of EB differs somewhat from the initially populated state. This can be attributed to the presence of the nitro groups in EB, which are known to have strong electron-withdrawing property. Therefore, the S_1 state of EB can be expected to have a substantial charge-transfer character. Because of this, the optical population of the Franck−Condon excited state must be followed by some ultrafast structural relaxation of high frequency modes. TD-DFT calculations performed on the dianionic form of EB confirm the charge-transfer character of the first electronic transition. They predict this transition to be at 2.5 eV and to be associated with a one-electron HOMO−LUMO transition which, as illustrated in Figure 4, involves a substantial increase of the electronic density on the nitro groups.

Additionally, the nitro groups can act as hydrogen-bond acceptors,[24−26] and, because of the higher electronic density in the S_1 state, H-bonds with surrounding solvent molecules should be stronger in the excited than in the ground state. The presence of hydrogen bonds between EB and solvent molecules could account for the broader emission spectrum in protic than in aprotic solvents as shown by the comparison of the fluorescence spectra recorded in MeOH and ACN (Figure 5A).

The absorption spectrum of EB in ACN differs significantly from that in protic solvents such as water and alcohols (Figure 5B). In particular, it exhibits an intense band around 425 nm that has to be attributed to a second, nonemissive, form of the dye, because it is not present in the fluorescence excitation spectrum recorded at 600 nm (Figure 5B). The latter closely resembles the absorption spectrum in water at high pH, whereas it differs from the absorption spectrum recorded in water at low pH. This indicates that in ACN, the doubly charged anion form of EB coexists with another one, most likely the neutral one, for the absorption spectra of lactones are typically located below 400 nm. Despite this coexistence, the properties of the doubly charged anion form of EB in ACN can be studied by time-resolved techniques because the absorption spectra of charged and neutral forms are well separated and, consequently, a given form can be selectively excited. Still, the presence of singly charged anions in addition to the doubly charged form cannot be entirely excluded, but their concentration must be low, because the band around 350 nm, intense in aqueous solution at pH = 3, where this form predominates, cannot be seen in ACN.

Transient Absorption (TA) Spectroscopy. TA spectra have been recorded upon 520 nm excitation of EB in water, MeOH,

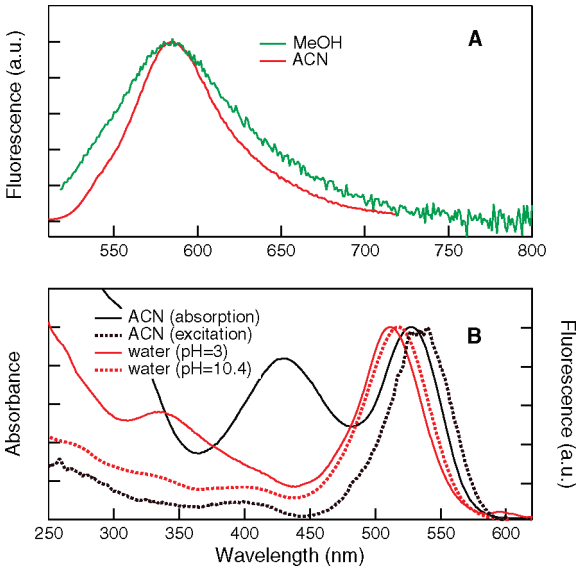

Figure 5. (A) Fluorescence spectra of EB in MeOH and ACN and (B) absorption spectra of EB in ACN, water at pH = 3 and 10, and fluorescence excitation spectrum of EB in ACN.

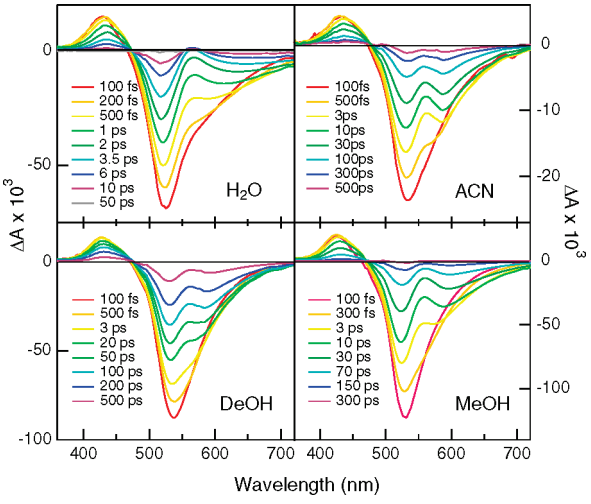

Figure 6. Transient absorption spectra recorded at different time delays after 520 nm excitation of EB in various solvents.

BuOH, DeOH and ACN (Figure 6, the data in BuOH are not shown as they are very similar to those in DeOH). The measurements have been carried out at 9×10^{-5} M EB concentration, but, as the spectral dynamics in water is the same at 10^{-5} M, one can conclude that aggregation does not play a significant role at these concentrations.

The TA spectra consist of three main bands: one extending from 360 to 470 nm due to excited-state absorption (ESA), a bleaching band coinciding with the $S_1 \leftarrow S_0$ absorption and a stimulated emission (SE) band, red-shifted with respect to the bleaching. In water and MeOH, the transient signals decay entirely within the temporal window of the experiment (500 ps), whereas the temporal evolution of the spectra in BuOH, DeOH, and ACN, although qualitatively very similar to that in MeOH, is slower and the transient signals do not vanish at the maximum time delay. Still, one can safely assume that in all solvents, the whole optically excited population relaxes directly

dx.doi.org/10.1021/jp110849x |J. Phys. Chem. A 2011, 115, 2465–2470

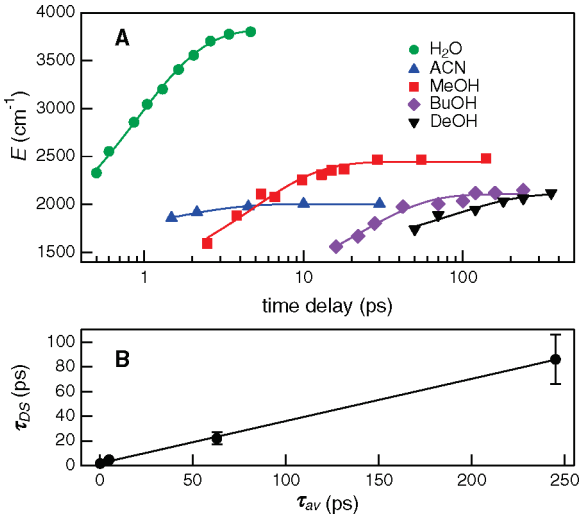

Figure 7. (A) Energy difference between the maxima of the SE and $S_1 \leftarrow S_0$ absorption bands of EB as a function of the time delay in various solvents. (B) Characteristic time τ_{DS} of the dynamic Stokes shift of EB vs the average correlation time of the solvents, τ_{av}.

Table 2. Time Constants Obtained from a Multi-Exponential Analysis of the Transient Absorption Data Recorded with EB in Various Solvents (τ_1–τ_3), Characteristic Time of the Dynamic Stokes Shift (τ_{DS}), and Average Correlation Time of the Solvent (τ_{AV})[27]

solvent	τ_1 (ps)	τ_2 (ps)	τ_3 (ps)	τ_{DS} (ps)	τ_{AV} (ps)
H_2O (3 exp.)	0.09[a]	1.0	4.3	0.89	
H_2O (2 exp.)		1.1	4.4		
D_2O (2 exp.)		1.6	7.6		
methanol	0.64	8.5	54	4.7	5
butanol	1.2	34	210	22	63
decanol	2.1	49	310	86	245
acetonitrile	2.6	23	280	1.6	0.26

[a] Shorter than the width of the response function of the TA setup.

to the ground state. Therefore, the fraction of molecules populating the triplet state is negligibly small.

The magnitude of the temporal shift of the SE band depends on solvent polarity: the more polar the solvent, the more red-shifted the emission at longer delays. The time dependence of the position of the SE band maximum can be well reproduced with a monoexponential function (Figure 7A). The time constant of this shift is directly proportional to the average correlation time of the solvent[27] (Figure 7B and Table 2), therefore this effect can be almost entirely attributed to the dynamic Stokes shift of the SE resulting from solvent relaxation. In contrast, the SE band of EY in water and alcohols, that can be seen as a shoulder between 560 and 620 nm, lies much closer to the bleaching band and does not shift in time (Figure 8). This indicates that the emitting state of EB is much more polar than that of EY and supports the hypothesis of its charge-transfer character introduced by the nitro substituents. The TA spectra recorded with EY in both water and MeOH exhibit very little spectral evolution within the temporal window of experiment, in agreement with a nanosecond excited-state lifetime.[12,14,28]

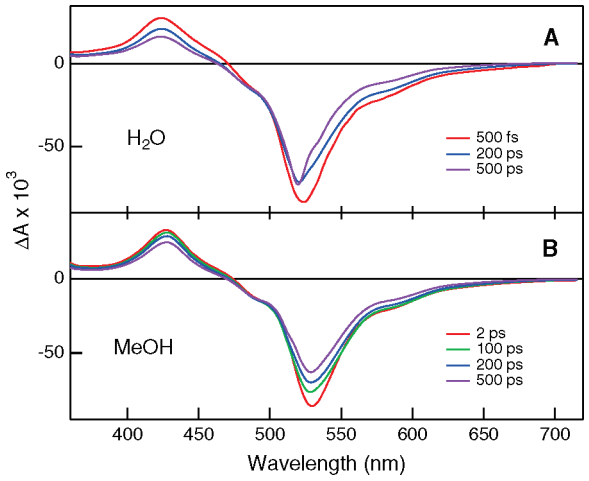

Figure 8. Transient absorption spectra recorded at various time delays after excitation at 520 nm of EY in water (A) and MeOH (B).

For EB, no other spectral evolution but the decay of the TA bands and the shift of the SE can be seen. In particular, there is no rise of any signals that could be attributed to build-up of the product of an excited-state reaction.

The excited-state lifetime of EB dramatically depends on the solvent: this dye is practically nonfluorescent in water, whereas its fluorescence can be clearly seen in ACN, BuOH, and DeOH when excited at 520 nm. In order to analyze quantitatively the dependence of the excited-state lifetime on solvent properties, TA profiles at three different wavelengths have been analyzed globally with multiexponential functions. The selected time profiles reflect the evolution of the signal at the maximum of the ESA band, at the maximum of the bleaching and close to the maximum of SE band, so that the influence of the shift of the latter is minimized. The three time constants required to satisfactorily reproduce the data are listed in Table 2 and the data together with the best-fit curves are presented in Figure S1 (see Supporting Information).

It is not possible to directly assign these time constants to a population transfer between different species or even to specific processes, like intramolecular vibrational redistribution or solvent relaxation, because the spectral evolution is dominated by nonexponential dynamics resulting from the dynamic Stokes shift. In this situation, the multiexponential analysis of the time profiles should be seen only as a numerical procedure performed to quantitatively describe the rate of the processes following optical excitation. Therefore, all three values have to be analyzed together and considered as a representation of the whole deactivation pathway, which includes vibrational and solvent relaxation and finally the excited-state decay. Only in an approximation, the two shorter time constants may be attributed to vibrational and solvent relaxation, whereas the longest time can be identified with the excited-state lifetime. The latter assignment is also reinforced by comparison with the fluorescence quantum yields (Table 1). Assuming that $\Phi_{fl} = k_{rad}\tau_3$ gives a rate constant of radiative deactivation, k_{rad}, ranging between 1 and 2×10^8 s^{-1}, depending on the solvent.

These time constants correlate with neither solvent viscosity nor polarity, but they correlate well with the strength of the solvent as a hydrogen-bond donor measured in both, the Kamlet–Taft, α,[29] and the Catalan–Diaz solvent acidity, SA,[30,31] scales.

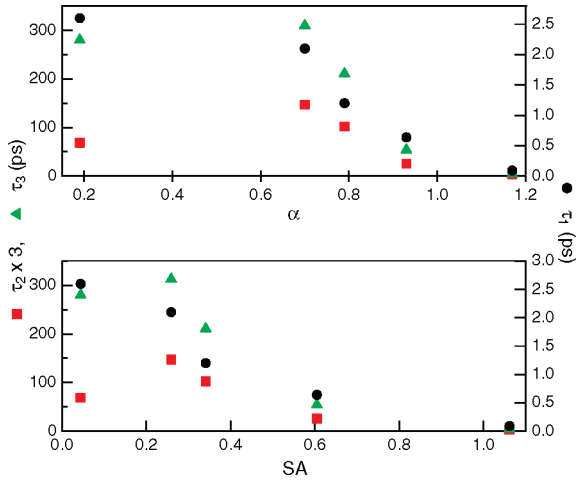

Figure 9. Time constants obtained from the analysis of the transient absorption data of EB vs (A) the Kamlet−Taft, α,[29] and (B) the Catalan-Diaz, SA,[30,31] parameters of the solvents (τ_2 has been multiplied by 3 for a better visualization).

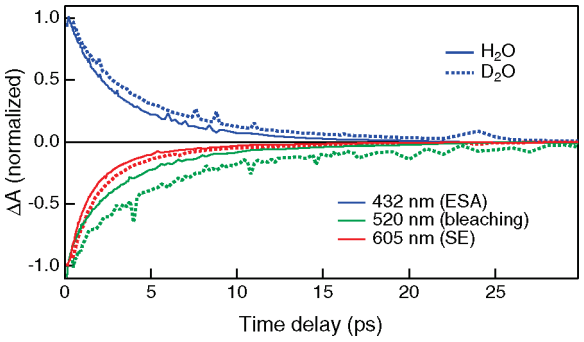

Figure 10. Transient absorption profiles measured with EB in H_2O and D_2O in the spectral regions of excited-state absorption (ESA), bleaching and stimulated emission (SE).

The correlation breaks down only with τ_2 in ACN. However, one has to remember that, in this case, the neutral form of EB might contribute to the TA signals. Besides this, the time profiles recorded in water and alcohols have a significant nonexponential component due to the dynamic Stokes shift of the SE band, whereas this effect is much weaker in ACN. The correlation between the time constants obtained from the TA data and both the α and SA parameters points to a key role of the hydrogen bonds in the excited-state deactivation.

The strong shortening of the excited-state lifetime of EB in protic solvents points to the occurrence of hydrogen-bond assisted nonradiatiave deactivation.[13,32−39] This process is enabled by the nitro groups of EB that are good hydrogen-bond acceptors.[24−26,40,41] In order to further confirm this hypothesis, TA measurements were carried out in perdeuterated water. As expected for the hydrogen-bond assisted deactivation mechanism, the dynamics in D_2O was slower than in H_2O (Figure 10) by approximately a factor 1.5 (Table 2).

In summary, we propose the following picture for the excited-state deactivation of EB in water and alcohols. The strength of the hydrogen bonds between the nitro groups and hydroxyl groups of the solvent increases upon optical excitation due to the charge transfer character of the transition and the rise of electron density on the nitro substituents. This in turn leads to an increase of the coupling with the solvent, enhancing the nonradiative deactivation. The exact mechanism of the hydrogen-bond assisted nonradiative deactivation is not totally understood. It could be thought in terms of an excited-state intermolecular proton transfer with the solvent molecules, followed by back proton transfer to the ground state. The absence of an intermediate in the TA spectra could be due to an incomplete proton transfer or to a back transfer that is much faster than the forward transfer.

Therefore, the excited-state lifetime of EB can be considered as a measure of the hydrogen-bonding properties of the environment. A scale of hydrogen-bond strength, analogical to the SA scale, could be based on either the fluorescence quantum yield or the excited-state lifetime of EB. Other xanthene dyes, namely rose Bengal and fluorescein, have already been demonstrated as probes for hydrogen bonds with the solvent.[42,43] In both dyes, hydrogen bonding with the solvent molecules results in a stabilization of the electronic states. This stabilization energy, whose magnitude depends on the nature of the excited state, leads to a change of the energy gap between these states, affecting the $S_1 \rightarrow T_1$ intersystem crossing rate constant of rose bengal,[42] and leading to a strong solvatochromism of the absorption band of fluorescein.[43] Therefore, either the fluorescence lifetime of rose Bengal or the absorption band maximum of fluorescein can be used as a scale of the hydrogen bond ability of the solvent.

EB differs considerably from the above dyes when applied as a hydrogen bonds probe. Its absorption spectrum depends weakly on the environment and only its excited-state lifetime changes with the solvent. Furthermore, its triplet state is not populated during the deactivation. Finally, the excited-state lifetime of EB (4.4 ps in water and 280 ps in ACN) is much shorter than that of rose Bengal (120 ps in water and 2.4 ns in ACN) and is also more sensitive to the hydrogen bond ability of the solvent, the ACN/water lifetime ratio being equal to 60 for EB and 20 for rose Bengal.

All of these features make EB particularly suitable for studying hydrogen bonds at interfaces by TRSSHG with femtosecond laser sources. In this technique, the population dynamics of various states of the probe dye is observed and the absence of triplet state population in the deactivation pathway of EB makes the interpretation of the data easier and more reliable. In turn, the weak influence of the solvent on the absorption spectrum of EB eliminates the changes of intensity of the generated second harmonic light, which strongly depends on resonances with electronic transitions of the dye. Furthermore, the time scale of the excited-state lifetimes matches very well the standard specifications of TRSSHG setups, which can readily reach subpicosecond temporal resolution. Therefore, EB can be applied as hydrogen bond probe in experiments where other probe molecules would fail or be very inconvenient to use.

CONCLUSIONS

This investigation reveals that, although structurally very similar, EB and EY have substantially different photophysics and excited-state dynamics. This difference stems from the charge-transfer character of the S_1 state of EB introduced by the presence of two nitro groups instead of bromine atoms. The increase of electronic density on these groups upon optical excitation is accompanied by a strengthening of hydrogen bonds in protic solvents. This is at the origin of the hydrogen-bond assisted nonradiative deactivation of the excited state of EB,

which decays within a few picoseconds in water and a few tens of picoseconds in methanol. Our results are quite consistent with the very short S_1-state lifetime of EB in methanol reported by Reindl et al.,[8] but depart totally from the nanosecond lifetimes reported in ethanol.[10,11] This discrepancy must most probably arise from a confusion between EB and EY, for which this hydrogen-bond assisted nonradiative deactivation is not operative.

As the excited-state lifetime of EB is directly related to the strength of the solvent as a hydrogen-bond donor, a corresponding scale based on the fluorescence quantum yield or lifetime could be built. Such a scale of hydrogen-bond strength would be most useful for the investigation of liquid/water or air/water interfaces using time-resolved second harmonic generation. Indeed, the ability of the interfacial molecules to make hydrogen bonds could be determined by measuring excited-state lifetime of EB at the interface. This idea will be demonstrated for liquid/water interfaces in a forthcoming work.[15]

■ ASSOCIATED CONTENT

Supporting Information. Transient absorption profiles of EB in various solvents at the maximum of the three main bands: excited-state absorption, bleaching, and stimulated emission. This material is available free of charge via the Internet at http://pubs.acs.org.

■ AUTHOR INFORMATION

Corresponding Author

*E-mail: Eric.Vauthey@unige.ch.

Present Addresses

†Institute of Experimental Physics, Faculty of Physics, University of Warsaw, ul. Hoza 69, 00−681 Warsaw, Poland

■ ACKNOWLEDGMENT

This work was supported by the Fonds National Suisse de la Recherche Scientifique through Project Nr. 200020-115942 and the NCCR-MUST, and by the University of Geneva. P.F. acknowledges the financial support of the Foundation for Polish Science.

■ REFERENCES

(1) Tamburello-Luca, A. A.; Hebert, P.; Antoine, R.; Brevet, P. F.; Girault, H. H. *Langmuir* **1997**, *13*, 4428.
(2) Antoine, R.; Tamburello-Luca, A. A.; Hébert, P.; Brevet, P. F.; Girault, H. H. *Chem. Phys. Lett.* **1998**, *288*, 138.
(3) Eisenthal, K. B. *Chem. Rev.* **1996**, *96*, 1343.
(4) Brevet, P.-F. *Surface Second Harmonic Generation*; Presses Polytechniques et Universitaires Romandes: Lausanne, 1997.
(5) Benjamin, I. *Chem. Rev.* **2006**, *106*, 1212.
(6) Shi, X.; Borguet, E.; Tarnovsky, A. N.; Eisenthal, K. B. *Chem. Phys.* **1996**, *205*, 167.
(7) Fita, P.; Punzi, A.; Vauthey, E. *J. Phys. Chem. C* **2009**, *113*, 20705.
(8) Reindl, S.; Penzkofer, A. *Chem. Phys.* **1996**, *213*, 429.
(9) Berlman, I. B. *Handbook of Fluorescence Spectra of Aromatic Molecules*; Academic Press: New York, 1971.
(10) Math, N. N.; Naik, L. R.; Suresh, H. M.; Inamdar, S. R. J. *Lumin.* **2006**, *121*, 475.
(11) Nijegorodov, N.; Mabbs, R. *Spectrochim. Acta A* **2001**, *57*, 1449.
(12) Wyatt, W. A.; Poirier, G. E.; Bright, F. V.; Hieftje, G. M. *Anal. Chem.* **1987**, *59*, 572.
(13) Flom, S. R.; Barbara, P. F. *J. Phys. Chem.* **1985**, *89*, 4489.
(14) Balzani, V.; Ceroni, P.; Gestermann, S.; Gorka, M.; Kauffmann, C.; Maestri, M.; Vogtle, F. *ChemPhysChem* **2000**, *1*, 224.
(15) Fita, P.; Fedoseeva, M.; Vauthey, E. *Langmuir*, in press.
(16) Kubin, R. F.; Fletcher, A. N. J. *Lumin.* **1982**, *27*, 455.
(17) Duvanel, G.; Grilj, J.; Schuwey, A.; Gossauer, A.; Vauthey, E. *Photochem. Photobiol. Sci.* **2007**, *6*, 956.
(18) Banerji, N.; Duvanel, G.; Perez-Velasco, A.; Maity, S.; Sakai, N.; Matile, S.; Vauthey, E. *J. Phys. Chem. A* **2009**, *113*, 8202.
(19) Perdew, J. P. *Phys. Rev. B* **1986**, *33*, 8822.
(20) Schäfer, A.; Horn, H.; Ahlrichs, R. *J. Chem. Phys.* **1992**, *97*, 2571.
(21) Bauernschmitt, R.; Ahlrichs, R. *Chem. Phys. Lett.* **1996**, *256*, 454.
(22) Ahlrichs, R.; Bär, M.; Häser, M. *Chem. Phys. Lett.* **1989**, *162*, 165.
(23) Levillain, P.; Fompeydie, D. *Anal. Chem.* **1985**, *57*, 2561.
(24) Urbanski, T. *Tetrahedron* **1959**, *6*, 1.
(25) Ungnade, H. E.; Roberts, E. M.; Kissinger, L. W. *J. Phys. Chem.* **1964**, *68*, 3225.
(26) Mohammed, O. F.; Vauthey, E. *J. Phys. Chem. A* **2008**, *112*, 3823.
(27) Horng, M. L.; Gardecki, J. A.; Papazyan, A.; Maroncelli, M. *J. Phys. Chem.* **1995**, *99*, 17311.
(28) Flom, S. R.; Fendler, J. H. *J. Phys. Chem.* **1988**, *92*, 5908.
(29) Taft, R. W.; Kamlet, M. J. *J. Am. Chem. Soc.* **1976**, *98*, 2886.
(30) Catalan, J.; Diaz, C. *Liebigs Ann. Chem.* **1997**, 1941.
(31) Catalan, J.; Diaz, C. *Eur. J. Org. Chem.* **1999**, 885.
(32) Inoue, H.; Hida, M.; Nakashima, N.; Yoshihara, K. *J. Phys. Chem.* **1982**, *86*, 3184.
(33) Yatsuhashi, T.; Inoue, H. *J. Phys. Chem. A* **1997**, *101*, 8166.
(34) Cser, A.; Nagy, K.; Biczok, L. *Chem. Phys. Lett.* **2002**, *360*, 473.
(35) Fürstenberg, A.; Vauthey, E. *Photochem. Photobiol. Sci.* **2005**, 260.
(36) Sherin, P. S.; Grilj, J.; Tsentalovitch, Y. P.; Vauthey, E. *J. Phys. Chem. B* **2009**, *113*, 4953.
(37) Nishiya, T.; Yamauchi, S.; Hirota, N.; Baba, M.; Hanazaki, I. *J. Phys. Chem.* **1986**, *90*, 5730.
(38) Banerji, N.; Fürstenberg, A.; Bhosale, S.; Sisson, A. L.; Sakai, N.; Matile, S.; Vauthey, E. *J. Phys. Chem. B* **2008**, *112*, 8912.
(39) Petkova, I.; Dobrikov, G.; Banerji, N.; Duvanel, G.; Perez, R.; Dimitrov, D.; Nikolov, P.; Vauthey, E. *J. Phys. Chem. A* **2010**, *114*, 10.
(40) Su, Y. S.; Hong, H. K. *Spectrochim. Acta A* **1967**, *24*, 1461.
(41) Granzhan, V. A.; Semenenko, S. V.; Zaitsev, P. M. *J. Appl. Spectrosc.* **1968**, *9*, 407.
(42) Cramer, L. E.; Spears, K. G. *J. Am. Chem. Soc.* **1978**, *100*, 221.
(43) Klonis, N.; Clayton, A. H. A.; Voss, E. W.; Sawyer, W. H. *Photochem. Photobiol.* **1998**, *67*, 500.